



ELSEVIER

Surface Science xxx (2002) xxx–xxx

SURFACE SCIENCE

www.elsevier.com/locate/susc

Stochastic approach to the smart quantum confinement model in porous silicon

A. Ramírez-Porras^{a,*}, S.Z. Weisz^b

^a Centro de Investigación en Ciencia e Ingeniería de Materiales and Escuela de Física, Universidad de Costa Rica, San Pedro 2060, Costa Rica, USA

^b Department of Physics and Materials Research Center, University of Puerto Rico, Río Piedras, PR 00931, USA

Received 22 March 2002; accepted for publication 10 June 2002

Abstract

A model that encompasses two approaches to explain the photoluminescence in p-type porous silicon is proposed. The model considers a stochastic distribution of nanocrystallite sizes within the porous matrix and explain the luminescence emission of air-exposed specimens in terms of the presence of Si=O and Si=H bonds. Fitting of experimental data is performed to extract size-related statistical parameters. The results are in good agreement with the band-to-band and localized state-to-band transition theoretical framework. © 2002 Published by Elsevier Science B.V.

PACS: 73.20.D; 73.20.Dx; 73.20.Hb; 73.50.M; 78.55

Keywords: Semiempirical model and model calculation; Electrochemical methods; Photoluminescence; Silicon; Silicon oxides; Quantum wells; Semiconducting films

The mechanism of photoluminescence (PL) in porous silicon (PS) has been a source of controversy since its discovery by Canham [1]. Many models have been proposed to explain the spectrum shape [2], but it is generally accepted that the PL emission follows a widening in the band gap due to the presence of nanocrystalline structures formed by the electrochemical etching process [3]. Raman studies [4–6] and XTEM [7] report the presence of spherical crystallites in the nanometer range (“quantum dots”, QD), although some SAXS measurements [8,9] are consistent with a

network of extended silicon quantum wires (QW). Recently, Wolkin and coworkers [10] proposed a comprehensive model which states that the PL spectra belonging to specimens held at ambient air are characteristic of transitions from localized-to-band states that lie deep in the band gap. They claim that the origin of these states come from the trapping of an electron (or an exciton) by silicon–oxygen bonds in nanocrystals smaller than 3 nm, but they do not provide further information on distribution sizes. In contrast, a study from John and Singh [11] describes a method to determine their structural parameters (diameter and variance). The purpose of this letter is to combine both approaches to deduce the size distribution of crystallites and their luminescent properties in PS samples.

* Corresponding author. Tel.: +506-2075394; fax: +506-2255511.

E-mail address: aramirez@hermes.efis.ucr.ac.cr (A. Ramírez-Porras).

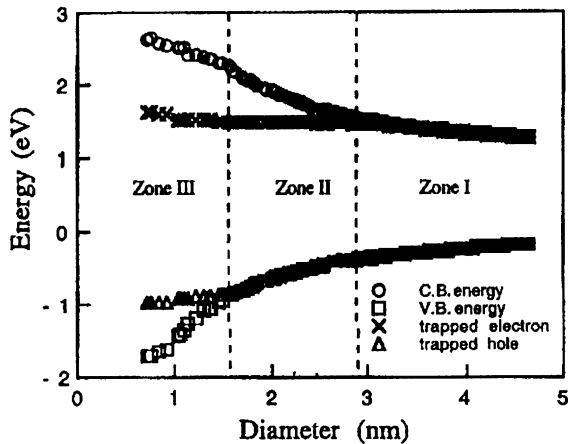


Fig. 1. Electronic states energy as function of crystallite size in PS exposed to ambient air. In zone I there is only influence of quantum confinement; in zone II an electron p-state on the silicon atom shows up; in zone III a hole p-state on the oxygen atom also arises (figure taken from Ref. [9]).

47 The theoretical model employed by Wolkin et
48 al. to calculate the electronic structure of silicon
49 clusters as a function of nanocrystalline QD sizes
50 for oxygen and hydrogen surface passivation uses
51 a self-consistent tight-binding method [12]. The
52 details are listed in Ref. [10]. The results from these
53 calculations are presented in Fig. 1. Three impor-
54 tant zones have been identified in the process of
55 recombination. Firstly, a zone for diameters larger
56 than ~ 3 nm where the recombination takes place
57 through free excitons, and therefore the PL spectra
58 is directly related with the band gap. Notice that in
59 this case, a reduction in the QD size results in an
60 enlargement of the gap and in the spectra blue
61 shift. Secondly, a zone for diameters between 2
62 and 3 nm where a trapped electron state arises.
63 This state seems to be a p-state in the silicon atom
64 of the Si=O bond. In this regime, recombinations
65 are performed between this trapped state and a
66 free hole from the valence band. As the QD size
67 decreases, the shift in PL spectra is towards the
68 blue but not as fast as in zone I. Lastly, a zone for
69 diameters lower than ~ 2 nm is characterized by
70 the presence of this silicon trapped state in addi-
71 tion to a new oxygen trapped state. The recombi-
72 nation process is consequently through trapped
73 excitons where no shift in the PL is observed. This
74 effect was also observed by Kanemitsu and co-

workers [13]. It is worth to point out that theo- 75
retical calculations rule out possible 76
recombinations through dangling bonds, at least 77
for the usual red PL [14]. 78

One of the drawbacks of the Wolkin's model is 79
that it does not account for a statistical distribu- 80
tion of crystallites sizes. Some studies propose a 81
Gaussian function [11,15,16] while others claim 82
that a log-normal distribution is more accurate 83
[17,18]. We assumed in this study a Gaussian-like 84
distribution function for the reasons that follow. 85

The stochastic model was originally proposed 86
by John and Singh [11], but later refined by Elh- 87
ouchet et al. [15]. Consider a Gaussian distribu- 88
tion of QD and QW nanostructures with 89
respective diameters d_d and d_w centered about 90
means d_{0d} and d_{0w} and with standard deviations σ_d 91
and σ_w . The distributions are: 92

$$P_d = \frac{1}{\sqrt{2\pi}\sigma_d} \exp \left[-\frac{1}{2} \left(\frac{d_d - d_{0d}}{\sigma_d} \right)^2 \right] \quad (1)$$

$$P_w = \frac{1}{\sqrt{2\pi}\sigma_w} \exp \left[-\frac{1}{2} \left(\frac{d_w - d_{0w}}{\sigma_w} \right)^2 \right] \quad (2)$$

The probability distribution of the PL process for 95
both QD and QW are: 96

$$P_d(\Delta E) = K_d (\Delta E)^{-3.88} \exp \left[-\frac{1}{2} \left(\frac{d_{0d}}{\sigma_d} \right)^2 \right] \times \left(\frac{c_d^{0.72}}{d_{0d}} (\Delta E)^{-0.72} - 1 \right)^2 \quad (3)$$

$$P_w(\Delta E) = K_w (\Delta E)^{-3.16} \exp \left[-\frac{1}{2} \left(\frac{d_{0w}}{\sigma_w} \right)^2 \right] \times \left(\frac{c_w^{0.72}}{d_{0w}} (\Delta E)^{-0.72} - 1 \right)^2 \quad (4)$$

where $K_{d,w}$ are normalization constants, and 99
 $\Delta E = c_{d,w}/d^{1.39}$ is the quantum confinement energy 100
($c_{d,w}$ are their associated constants) [14]. ΔE is re- 101
lated with the PL energy ($h\nu$), the bulk silicon gap 102
($E_g \sim 1.15$ eV) and the exciton binding energy 103
($E_b \sim 0.15$ eV) by: $\Delta E = h\nu - (E_g - E_b) \approx h\nu - 1$ 104
(eV). The PL spectrum shape is therefore a 105
weighted addition of these two expressions plus a 106

107 contribution from the localized-to-band state
 108 proposed by Wolkin et al. and applicable for zones
 109 II and III. It will also be assumed a Gaussian like
 110 contribution in the form:

$$P_{\text{loc}}(\Delta E) = K_{\text{loc}} \exp \left[-\frac{1}{2} \left(\frac{(\Delta E) - (\Delta E)_0}{\sigma_{\text{loc}}} \right)^2 \right] \quad (5)$$

112 where K_{loc} is a normalization constant, $(\Delta E)_0$ the
 113 mean of the distribution and σ_{loc} its standard de-
 114 viation.

115 Our PS samples were prepared by usual electro-
 116 chemical etching in HF:EtOH aqueous solution
 117 in the proportion 1:1 on boron-doped, (100)
 118 crystallographic plane and 30–50 Ωcm resistivity
 119 wafers. The current density was kept at 100 mA/
 120 cm^2 in all cases, and the time of the etching process
 121 were from 2 to 30 min. The PL was determined in
 122 air at room temperature after rinsing and drying
 123 by the use of a fiber optics, CCD-based spectro-
 124 photometer with a He–Cd 442 nm, 1 mW laser as a
 125 light source. An optical band-pass filter was em-
 126 ployed to filter out the laser plasma lines. Fig. 2
 127 shows typical spectra from these samples. Once the
 128 spectra were recorded and stored in a computer
 129 system, a Gaussian fitting procedure software was

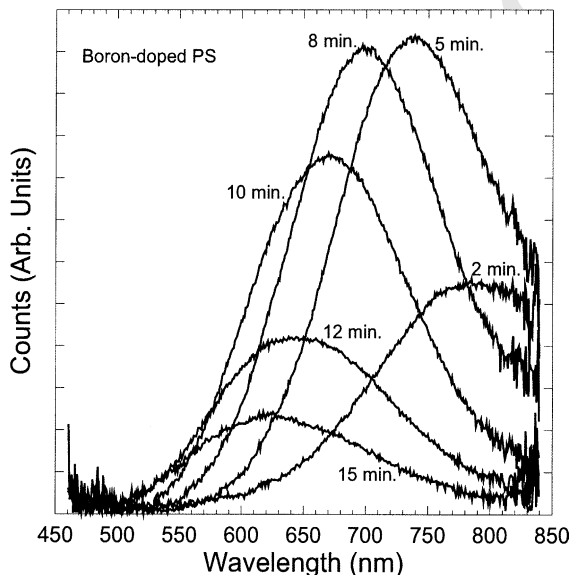


Fig. 2. PL spectra for various electrochemical etching times, as marked in the figure. Notice a blue shift in the maximum peak of the spectra for increasing times.

130 employed to first determine the statistical param-
 131 eters of Eqs. (3) and (4), assuming initially that
 132 only QD and QW were responsible for the ob-
 133 tained PL. With the mean diameters extracted
 134 from the fitting method, it was decided whether the
 135 actual PL spectrum belonged to zone I, II or III
 136 (see Fig. 1). If zone I was selected, then no local-
 137 ized-to-band transition was considered and the
 138 process stopped. If zone II was selected, a new
 139 fitting process was performed with the additional
 140 presence of localized states. None of our samples
 141 were attributed to zone III due to the obtained
 142 values of d . Statistical parameters of Eqs. (3)–(5)
 143 were therefore extracted. Typical fits from PL
 144 spectra of zones I and II are shown in Fig. 3.

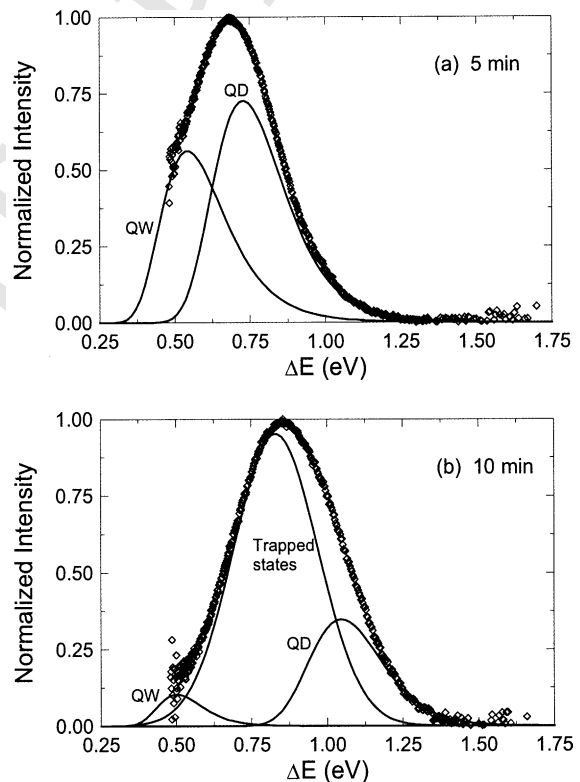


Fig. 3. Typical PL spectra as a function of ΔE for 5 min (a) and 10 min (b) etching time. In (a), only the contributions of QD and QW are sufficient to fit the experimental data, which is characteristic of zone I. In (b), a taller Gaussian peak (attributed to trapped states and characteristic of zone II) is necessary to fit the data. QD and QW contribution are notably smaller but still present. The statistical parameters of both cases are listed in Table 1.

Table 1
Statistical parameters extracted from the fitting procedure

Sample label	Etching time (min)	Zone	d_{0d} (nm)	σ_d (nm)	d_{0w} (nm)	σ_w (nm)	$E_{0,loc}$ (eV)	$\sigma_{0,loc}$ (eV)
S1-02	2	I	3.16	0.64	4.59	0.16	–	–
S1-05	5	I	3.04	0.40	4.09	0.66	–	–
S1-08	8	II	2.77	0.42	3.66	0.87	1.77	0.16
S1-10	10	II	2.55	0.22	4.56	0.52	1.83	0.14
S1-12	12	II	2.25	0.22	4.19	1.81	1.87	0.16
S1-15	15	II	2.23	0.24	3.70	0.14	1.98	0.23
S2-10	10	II	2.77	0.35	4.67	0.01	1.65	0.19
S2-15	15	II	2.55	0.49	3.60	0.69	1.86	0.16
S2-20	20	II	2.27	0.18	3.58	0.61	1.92	0.20
S2-25	25	II	2.21	0.18	3.43	0.34	1.92	0.25
S2-30	30	II	2.12	0.24	3.92	0.40	1.86	0.16

d_{0d} , σ_d , d_{0w} and σ_w are related with the QD and QW crystallites, respectively. $E_{0,loc}$ and $\sigma_{0,loc}$ are the actual mean energy and the standard deviation of the expected localized-to-band transitions, respectively.

145 The statistical results from these fittings are
 146 presented in Table 1 for two sets of samples. It
 147 is noticeable the reduction of crystallite size as the
 148 etching time increases. This agrees well with the
 149 blue shift that predicts the quantum confinement
 150 model. From the data of d_{0d} it is possible to cal-
 151 culate the mean quantum confinement energy ΔE
 152 and the peak PL energy from $h\nu \approx \Delta E + 1$ (eV).
 153 Fig. 4 shows the plot reported by Wolkin's group

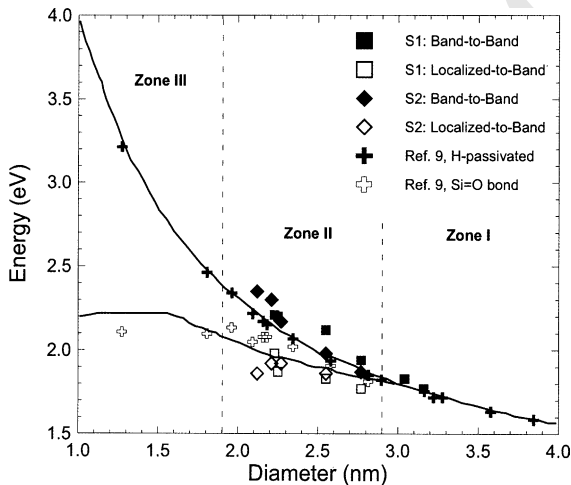


Fig. 4. PL energy as a function of crystallite diameter for theory (solid lines) and experimental results. The full and empty crosses come from Ref. [9], and the squares are our results. The full symbols consider radiative band-to-band recombinations, whereas the empty symbols represent localized-to-band recombinations.

[10] but with our results added. The figure does not
 include standard deviation bars (corresponding to
 the σ values) to avoid confusion. The curves cor-
 respond to the theoretical cases deduced for
 spherical crystallites, and therefore we only show
 the results for QD (QW mean diameters lie outside
 the plotted region in any case, and its contribution
 is a subject of a further study not included here).
 The agreement between the experimental points
 and the theoretical curves is notable. Full symbols
 represent band-to-band transitions where the PL
 emission is explained by pure quantum confinement.
 Empty symbols are localized-to-band transitions
 explained by the presence of Si=O bonds. The fact
 that for every situation depicted in Table 1 there
 is a coexistence of both kinds of transitions may
 be surprising at first glance. We attribute this
 duality to the following: after being exposed to
 ambient air, the nanostructures are partially
 passivated with H bonds and partially with O
 bonds [19]. As a consequence, depending on the
 proportion of Si=O to Si-H bonds, there must be
 two competing channels of radiative recombina-
 tion. The observed PL spectrum is indeed the
 result of these two processes.

In summary, a unified model accounting for the
 Si=O trapped state approach and the stochastic
 distribution of nanocrystal sizes approach has
 been proposed. The results for QD are in good
 agreement with previous published theoretical
 results and indicate that the mayor part of the PL

154
155
156
157
158
159
160
161
162
163
164
165
166
167
168
169
170
171
172
173
174
175
176
177
178
179
180
181
182
183
184

185 spectra comes from transitions from localized-to-
 186 band states and, in lesser extent, from band-to-
 187 band, at least in zone II. These results support
 188 therefore the so-called smart quantum confine-
 189 ment model even in the presence of stochastic os-
 190 cillations of nanostructure sizes.

191 References

- 192 [1] L.T. Canham, Appl. Phys. Lett. 57 (1990) 1046. 205
 193 [2] See a review in O. Bisi, S. Ossicini, L. Pavesi, Surf. Rev. 206
 194 Rep. 38 (2000) 1. 207
 195 [3] C. Delerue, G. Allan, M. Lannoo, J. Lumin. 80 (1999) 65. 208
 196 [4] Z. Sui, P.P. Leong, I.P. Herman, G.S. Higashi, H. Temkin, 209
 197 Appl. Phys. Lett. 60 (1992) 2086. 210
 198 [5] H. Münder, C. Andrzejak, M.G. Berger, U. Klemradt, H. 211
 199 Lüth, R. Herino, M. Ligeon, Thin Solid Films 221 (1992) 212
 200 27. 213
 201 [6] R.K. Soni, L.F. Fonseca, O. Resto, S.Z. Weisz, S. 214
 202 Tripathy, Mat. Res. Soc. Symp. Proc. 571 (2000) 235. 215
 203 [7] M.H. Nayfeh, Z. Yamani, O. Gurdal, A. Alaql, Mat. Res. 216
 204 Soc. Symp. Proc. 536 (1999) 191. 217
 [8] V. Lehmann, B. Jobst, R. Muschik, A. Kux, V. Petrova- 218
 Koch, Jpn. J. Appl. Phys. 32 (1993) 2095. 219
 [9] A. Naudon, P. Goudeau, V. Vezin, in: J.C. Vial, J. Derrien 220
 (Eds.), Porous Silicon Science and Technology, Les 221
 Editions de Physique, Paris, 1995. 222
 [10] M.V. Wolkin, J. Jorne, P.M. Fauchet, G. Allan, C. 223
 Delerue, Phys. Rev. Lett. 82 (1999) 197, Mat. Res. Soc. 224
 Symp. Proc. 536 (1999) 185. 225
 [11] G.C. John, V.A. Singh, Phys. Rev. B 50 (1994) 5329. 226
 [12] M. Lannoo, J. Bourgoin, in: M. Cardona (Ed.), Point 227
 Defects in Semiconductors, Springer-Verlag, New York, 228
 1981. 229
 [13] Y. Kanemitsu, H. Mimura, T. Matsumoto, T. Nakamura, 230
 J. Lumin. 72-74 (1997) 344. 231
 [14] C. Delerue, G. Allan, M. Lannoo, Phys. Rev. B 48 (1993) 232
 11024. 233
 [15] H. Elhouichet, B. Bessaïs, O. Ben Younes, H. Ezzaouia, M. 234
 Oueslati, Thin Solid Films 304 (1997) 358. 235
 [16] H.S. Mavi, B.G. Rasheed, R.K. Soni, S.C. Abbi, K.P. Jain, 236
 Thin Solid Films 397 (2001) 125. 237
 [17] H. Yorikawa, S. Muramatsu, J. Lumin. 87 (2000) 423. 238
 [18] S. Miyazaki, A. Mouraguchi, K. Shiba, Thin Solid Films 239
 297 (1997) 183. 240
 [19] T. Tsybeskov, P.M. Fauchet, Appl. Phys. Lett. 64 (1994) 241
 1983. 242

UNCORRECTED